HIGH TEMPERATURE OXIDATION OF SPONGE-BASED E110 ALLOY IN AIR

PAVEL VRBKA
Department of Nuclear Reactors, Faculty of Nuclear Sciences and Physical Engineering, CTU in Prague, V Holešovičkách 2, 180 00 Praha 8

JAKUB KREJČÍ, JITKA KABÁTOVÁ, JAKUB KOČÍ, FRANTIŠEK MANOCH, VĚRA VRTÍLKOVÁ
UJP PRAHA a.s., Nad Kamínkou 1345, 156 10 Praha – Zbraslav

ABSTRACT

The work is focused on separate-effect testing of high temperature oxidation of sponge based E110 alloy in air environment. A dependence of weight gain on exposure time and other post-experimental evaluation as is length growth, cross-section metallography, microhardness, ring compression tests were investigated in temperature range 700–1200 °C. Pre-oxidized samples were prepared as well using autoclave oxidation methodology. A protective pre-oxidation effect and an influence of flow rate on high temperature air oxidation results were examined in temperature range 800–1200 °C. Based on experimental results of weight gain measurements for sponge-based E110 alloy, correlations for the oxidation kinetics were determined in pre- and post-breakaway region.

1 Introduction

A fuel cladding is one of four barriers protecting the environment against a leakage of radioactive materials appearing in nuclear reactors. Severe accidents like in past Three Mile Island (1979) or mainly Fukushima Daichi (2011) made possible to interaction between the cladding and air after a melting core leading to reactor vessel failure or a loss of cooling accident in a spent fuel pool. It was a reason why this phenomenon began to be examined. Since a lot of experiments was carried out under various conditions. In ANL was performed an experiment with short specimens of Zircaloy-4, ZIRLO and M5 cladding during low-temperature air oxidation [2]. Similar experiment was carried out in IRSN [5] with Zircaloy-4 and M5 alloy. In KIT were made two types of tests. The QUENCH-10 and QUENCH-16 [6] were focused on examination of a cladding bundle in simulated conditions of a loss-of-coolant accident with air ingress into core. Next there were performed series of separate-effect tests with short specimens during isothermal and non-isothermal conditions in air or mixture air-steam [1], [4]. Next research institutions are AEKI [7], PSI, UJP PRAHA a.s. etc. All investigations lead to same qualitative results. It was showed that air oxidation is significantly worse than steam or pure oxygen oxidation due to presence of nitrogen. Nitrogen reacts with alloy appearing nitrides, which are re-oxidized by a new oxygen and it leads to different internal tension in oxide layer and cracking. Due to cracks an oxidation rate increases. The increase is dependent on not only temperature but on effect of pre-oxidation, flow rate, atmosphere composition etc. too. Generally, there are pre-breakaway (parabolic kinetics) and post-breakaway (linear kinetics) area. Reaction rate is determined by Arrhenius equation, from which weight gain m^n_{ox} respective theoretic oxide thickness can be evaluated.

$$\frac{d\left(m_{ox}^{n}\right)}{dt} = A \cdot e^{\frac{-B}{T}} \tag{1.1}$$

Parameters *A, B* and reaction exponent *n* are dependent on specific conditions. The aim of all experiments is to gain these parameters for most of various situations, alloys and wide temperature range and it can be implemented in computational codes for modeling of severe accidents.

In this paper specimens of sponge-based E110 alloy were investigated especially weight gain, oxide layer, change of the shape, microstructure and mechanical properties. There was examined an influence of pre-oxidation and air flow rate too.

2. Experiment conduct

Experimental apparatus was set according to Fig. 1.

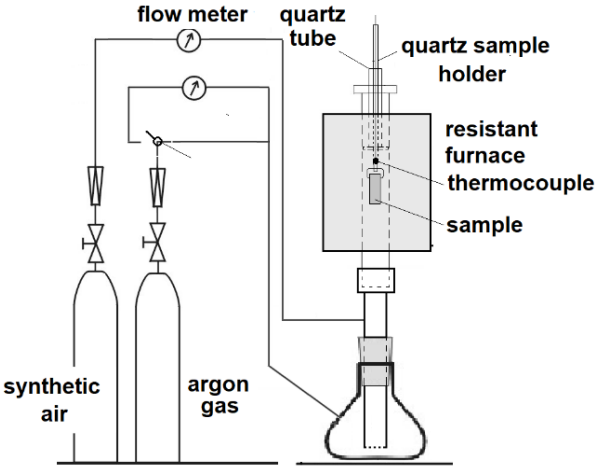

Fig. 1: Experimental apparatus for high temperature oxidation of E110 alloy in air

Oxidation was performed in a resistant furnace with a temperature regulation device up to 1200 °C. A sample of the cladding was hanged on a quartz stamen with a thermocouple in the end of the stamen. The furnace was connected with a flask by a quartz tube going through the furnace with a rubber plug. In the flask a stainless-steel tube was situated for a capture of the sample. A synthetic air and argon flowed through flow meters into the flask, where they were mixed each other and flowed vertically into the furnace around the sample.

At the beginning temperature was set on desired value and a temperature scale was measured along the height of the furnace for a position determination, where was desired temperature ± 3 °C. This position was set by handle of the quartz specimen holder. A display temperature on the PC had to be corrected for a temperature difference between the middle of the sample and a position of the thermocouple. After it prepared sample was hanged on the quartz tube, the flask was sealed by the plug and 10 l/min of argon switched on for an elimination of atmospheric air. After 5 minutes the oxidizing mixture of 18 l/h air and 6 l/h argon was set up for 10 minutes. Then the sample was pulled up into the furnace for oxidation. An exposure time was counted since the temperature overtake a three degrees lower value than desired one. After the exposure time the sample was pulled down and cooled by 10 l/min argon. The oxidized sample was weighted and measured again for the weight gain and extension determination. Then the sample was taken a photo and cut into rings. First 5mm one was poured into resin and polished for metallography examination, second one was tested for a hydrogen content and the ring compression test was performed with the last 7mm one.

There were examined three types of specimens of E110 alloy:

- as-received samples without any adjustments
- in-autoclave pre-oxidized samples in steam at 425 °C, 10,7 MPa for 42 days (5 μm) and 105 days (9,2 μm)
- high-temperature pre-oxidized samples in 2.8 l/h steam at 800 °C, 1000 °C, 1200 °C before air oxidation for oxide thickness 5 μm, 10 μm, 20 μm, 100 μm

3. Results

3.1. Weight gain

After exposure time specimens were weighted and weight gain was determined by a subtraction from prime weight. In Fig. 2 and Fig. 3 results for all sets of samples are displayed and compared each other. Due to error in a setting of the temperature correction real temperatures were slightly higher than desired ones. However, all text uses rounded values 700 °C, 800 °C etc. meaning 712 °C, 814 °C etc. in real.

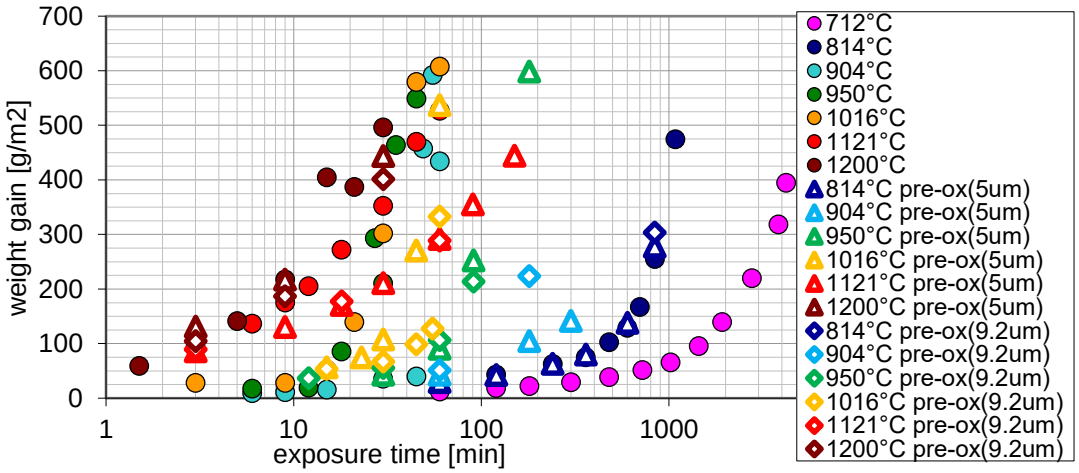

Fig. 2: Weight gain of as-received and in-autoclave pre-oxidized samples of cladding of E110 alloy after high temperature oxidation in air.

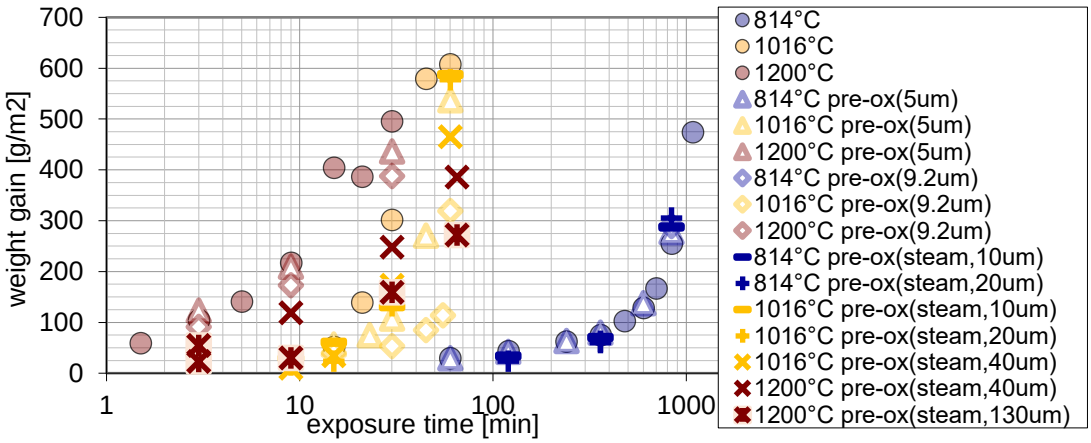

Fig. 3: Weight gain of as received, in-autoclave and high-temperature pre-oxidized samples of cladding of E110 alloy after high temperature oxidation in air.

The weight gain rapidly increased with temperature. As illustrated two regions of oxidation can be identified up to 1000 °C – parabolic pre-breakaway and linear post-breakaway area. For critical temperatures 900–1000 °C it sharply rose in post-breakaway area. In case of 900 °C there was significant scattering due to various breakaway time of particular samples. From

1100 °C no breakaway was observed and weight gain for longer exposition was lower than in case of lower temperatures due to its rapid oxidation after breakaway.
An influence of flow rate was investigated with 6 l/h air + 2 l/h argon and 30 l/h (resp. 40 l/h) + 10 l/h argon at 800 °C and 1100 °C. It was proved that for lower temperature weight gain declined with rising flow rate due to a local oxygen starvation. On the contrary for higher temperature it slightly increased due to a global oxygen starvation.
Pre-oxidation led to lower weight gain and later breakaway effect for the critical temperatures. Higher thickness of in-autoclave pre-oxidized samples gave lower weight gain except of 800 °C and 1100 °C. Protective effect had high-temperature pre-oxidation in steam only for 1200 °C. For 800 °C no difference was observed for all ways of pre-oxidation.

3.2. Visual inspection

Specimens were taken a photo for a visual comparation as you can see in Fig. 4 and Fig. 5 for as-received vs. pre-oxidized samples.

Fig. 4: Visual comparation of as-received cladding specimens of E110 alloy after high temperature oxidation in air.

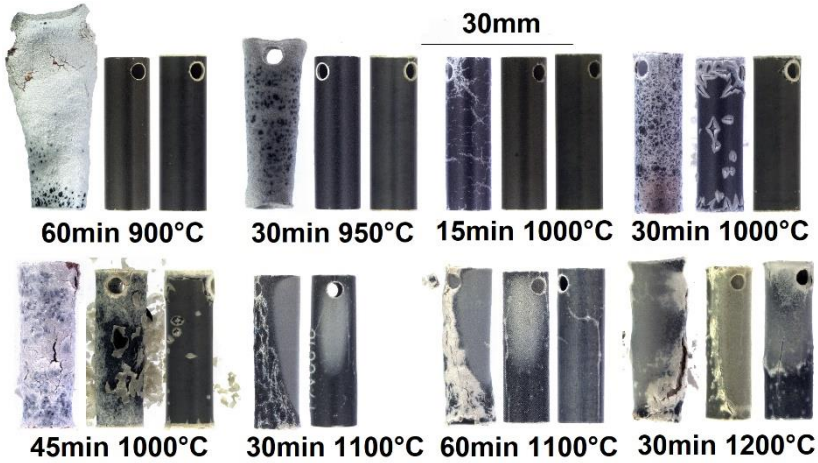

Fig. 5: Visual comparation of as-received cladding specimens of E110 alloy (left) with pre-oxidized ones in autoclave for 5 μm (middle) and 9,2 μm (right) after high temperature oxidation in air.

At first a dark compact oxide layer appeared. The local attack of nitrogen led to white cracks appearance. A density of cracks on the surface grew up and the oxide layer going to be light. For 950 °C the last specimen was totally oxidized and crumbled. A brown color maybe were residual nitrides. 800 °C specimens had a significant axial extension opposite of 1200 °C ones. Expressive extension was observed up to 950 °C. For higher temperatures it was negligible. The extension was caused by oxidation creep of α-Zr. Due to phase transformation to β-Zr for higher temperatures the extension became short. For 1100 °C and 1200 °C different oxide layer along specimens was observed due to global oxygen starvation. This effect is typical for

very high temperatures and insufficient flow rate when all oxygen is consumed and residual part of the sample is exposed only to nitrogen which is relatively inert.
The comparison in Fig. 5 gives a very clear difference between both sets of specimens. For same temperature and exposure time in-autoclave pre-oxidized samples were in a better condition than as-received ones. It was consistent with the weight gain measurement. Difference between two thicknesses was evident only for 1000 °C. In given image for 1100 °C global oxygen starvation for 9,2 μm was not recognized probably due to thick oxide layer.

3.3. Metalography

After cutting, pouring into resin and polishing the sample was examined under an optical microscope for a microstructure investigation. Comparison of metallographic cuttings of as-received and pre-oxidized samples is showed in Fig. 6 and Fig. 7.

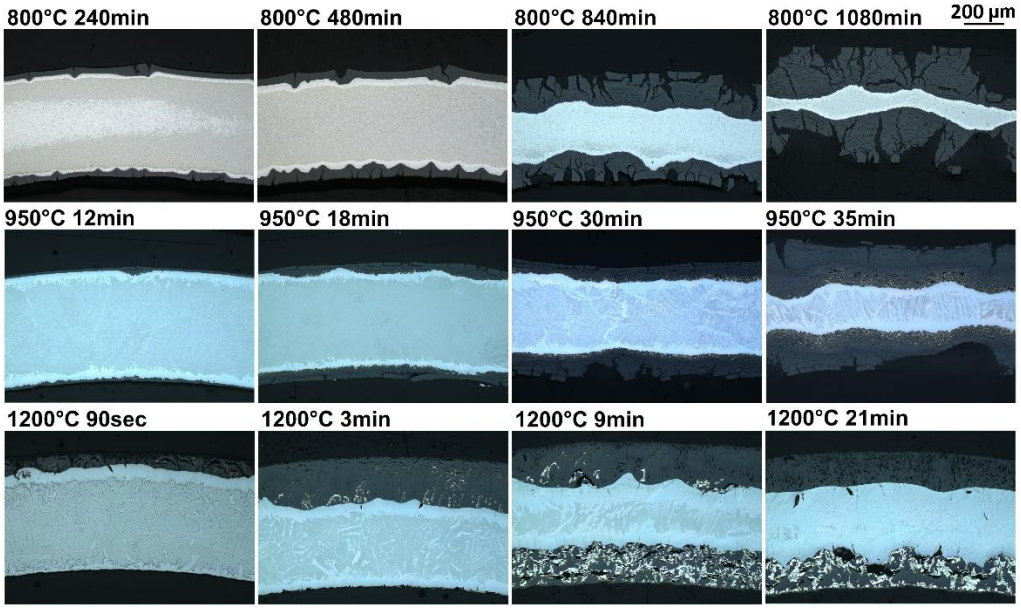

Fig. 6: Metallographic cuttings comparison of as-received cladding specimens of E110 alloy after high temperature oxidation in air.

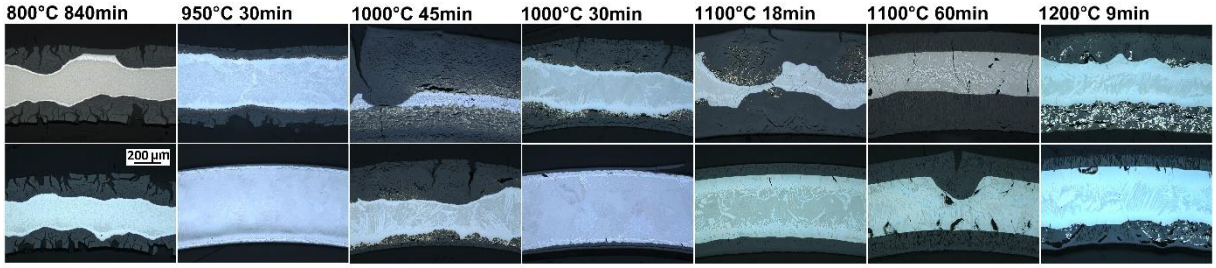

Fig. 7: Metallographic cuttings comparison of as-received cladding specimens of E110 alloy (up row) with pre-oxidized ones in autoclave for 5 μm (down row) after high temperature oxidation in air.

Columns in Fig. 6 were chosen for equivalent weight gain. With rising exposure time the oxide thickness grew, local nitrogen attack with cracks appeared and they were still numerous. It was the same observation as in case of visual inspection. Moreover, there were investigated an occurrence of stabilized α-Zr(O) phase and nitrides formation. It was shown that with increasing exposure time and with temperature the thickness of the phase increased. Due to higher diffusivity and solubility of oxygen in the alloy in higher temperature the phase was

observed in typical needle-shaped grains across the wall. For 800 °C the grains of nitrides were unrecognizable. For 950 °C they were small and relatively equally distributed near the boundary of oxide and metal. Bigger ones were observed for 1100 °C and 1200 °C. In outer oxide layer they were localized in nodules and in inner layer they were homogenously distributed in a higher concentration due to a lower flow. For 1200 °C and longer exposure times any nitrides were seen probably due to re-oxidation all of them. This phenomenon appears in case of samples where all metal in α-Zr(O) phase. There was only stochiometric oxide but nitrogen reacts mainly with non-stochiometric one which appears due to continuing diffusion of oxygen into metal [4].

Thickness of the metal wall was obviously higher in case of pre-oxidized samples except of 800 °C. In comparison with as-received ones there were a significantly less nitrides concentration and a bit more α-Zr(O) phase in higher temperatures.

Due to position of metallographic cutting there were a compact and uniform dense oxide layer without nitrides in case of 1100 °C and 1200 °C. This position was influenced by the global oxidation starvation. It is important to notice that the cuttings do not report about whole specimen properties. Images around all cutting were taken and there were seen that the wall was totally oxidized in the area uninfluenced by the oxygen starvation opposite of the influenced one.

3.4. Microhardness

In the middle of the wall Vickers microhardness was measured in 20 points around the metallographic cross-section. Mean values were brought into a chart in Fig. 8.

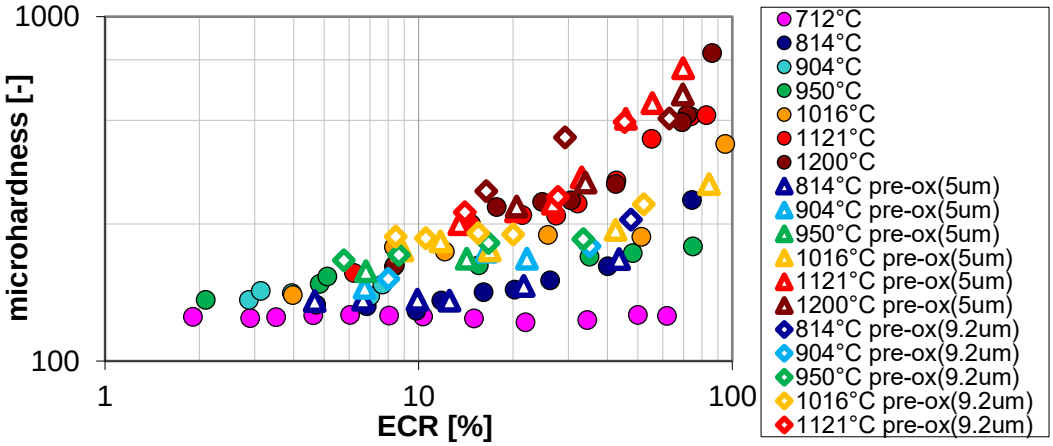

Fig. 8: Vickers microhardness of as-received and in-autoclave pre-oxidized cladding specimens of E110 alloy after high temperature oxidation in air.

Microhardness rose with rising temperature and ECR. The growth is significant only for higher temperatures. It was caused by a higher diffusivity and solubility of oxygen and subsequent hard α-Zr(O) phase formation as it was shown in the chapter before. In lower temperatures there was relatively uniform layer of the phase in the border on oxide and metal. No needle-shaped grains of the phase were observed up to 900 °C.

Microhardness of pre-oxidized samples was slightly higher due to the previously mentioned higher content of α-Zr(O) phase.

3.5. Ring compression test (RCT)

After cutting of an oxidized specimen one of rings was tested for a pressure deformation using INSTRON 1185 R5800 device. Deformation curves were gained and analyzed for a maximal load, ductility and total energy of deformation. Many of tests were finished before crack of the

sample. That is why ductility and energy were calculated in many cases for final deformation, signed “higher than calculated value”. Comparation of deformation curves for as-received and in-autoclave pre-oxidized specimens is shown in Fig. 9.

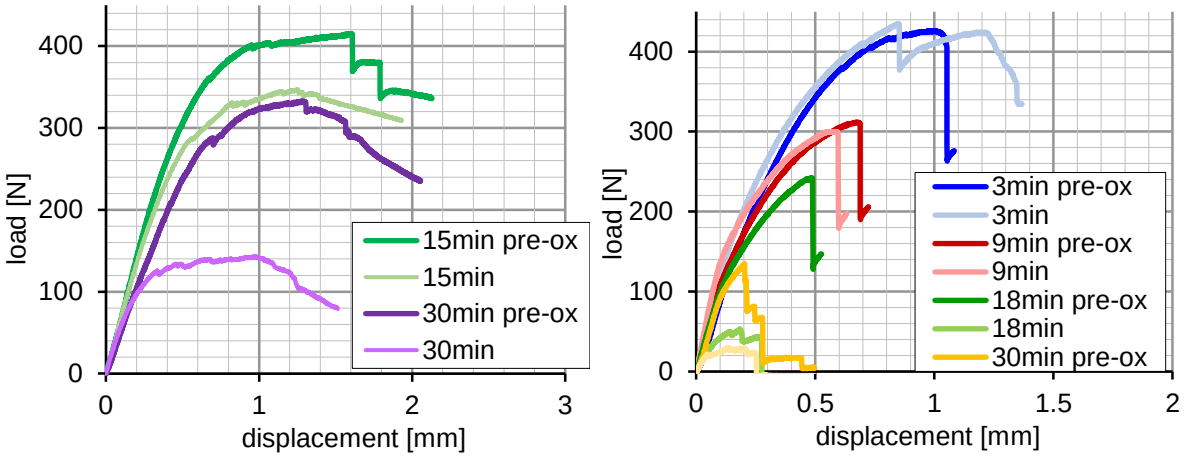

Fig. 9: RCT deformation curves comparation between as-received and in-autoclave pre-oxidized cladding specimens of E110 alloy after high temperature oxidation in air for two temperatures.

For all temperatures the maximal load gradually declined with growing ECR. Only for 1100 °C the load firstly slightly rose due to quick α-Zr(O) phase formation. A small fall in some deformation curves were caused by a crack of oxide layer. As shown in Fig. 9 the pre-oxidation effect improved mechanical properties – maximal load and total energy of deformation (area under the curve). These results agreed with metallographic cross-sections where a thinner metal wall was observed for as-received samples.

3.6. Hydrogen content

Content of hydrogen for as-received samples was 4–46 ppm depending on temperature. Values were slightly more for higher temperatures and different for various exposure times. The content for in-autoclave pre-oxidized up to 5 μm was 17–32 ppm and up to 9,2 μm was 160–180 ppm. For high-temperature pre-oxidized ones the measurement was not carried out yet.

4. Results comparation

Measured weight gains were compared with results other mentioned experiments performed in KIT, ANL and AEKI with Zircaloy-4, ZIRLOTM, M5 alloys. According to correlations in [3] for computational codes ASTEC and MELCOR 2.1 oxidation in air was modeled. Comparison with KIT and AEKI results is illustrated in Fig. 10–12 and comparison with the codes in Fig. 13.

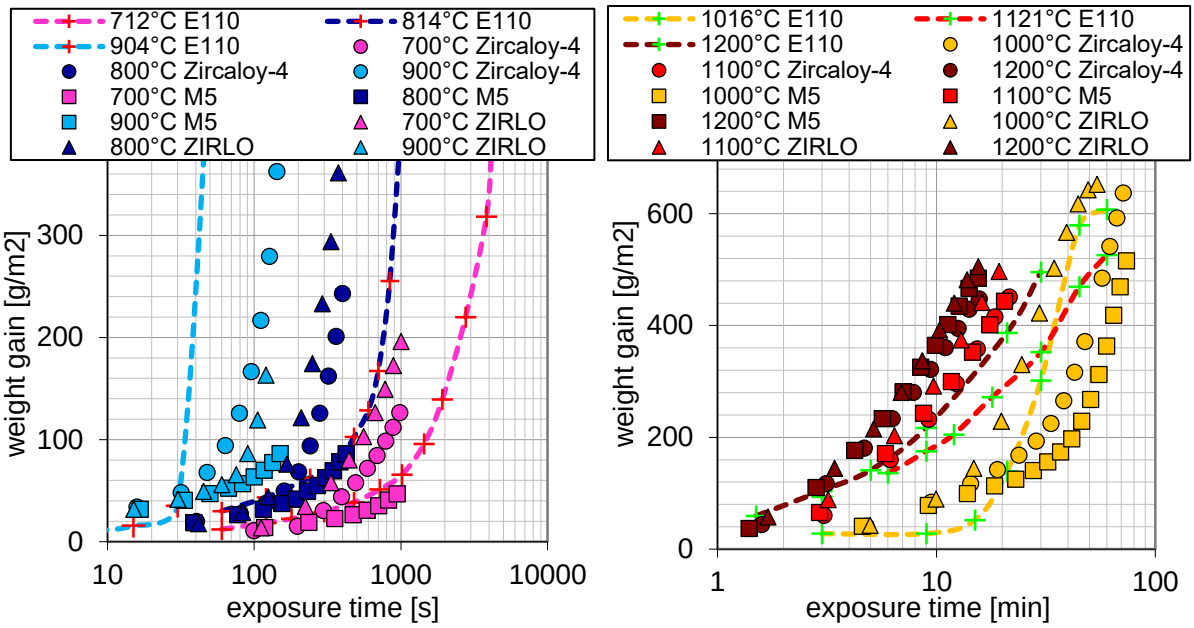

Fig. 10: Weight gain comparison of examined as-received E110 alloy with results of KIT [1] experiments with Zircaloy-4, ZIRLO™ and M5 alloys.

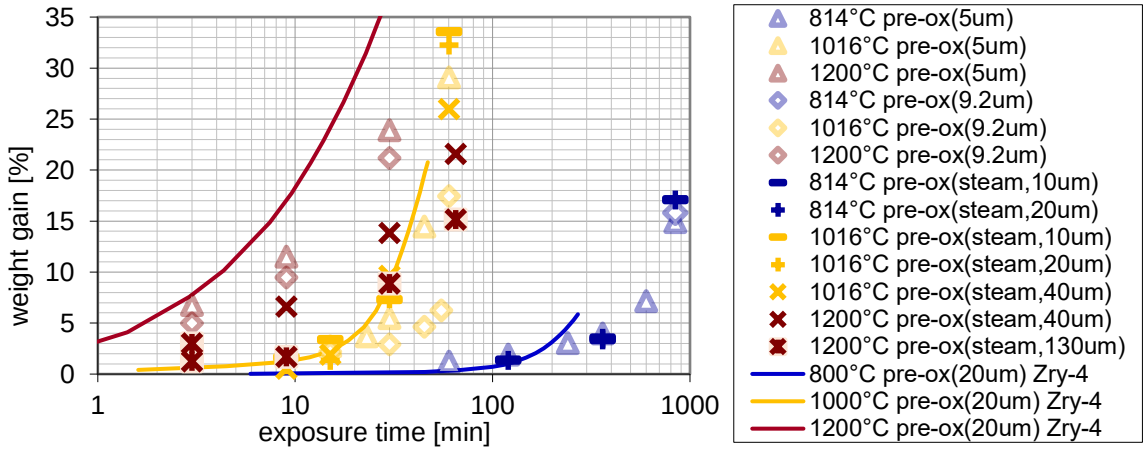

Fig. 11: Weight gain comparison of examined high-temperature pre-oxidized E110 alloy with results of KIT [4] experiments with Zircaloy-4 alloys.

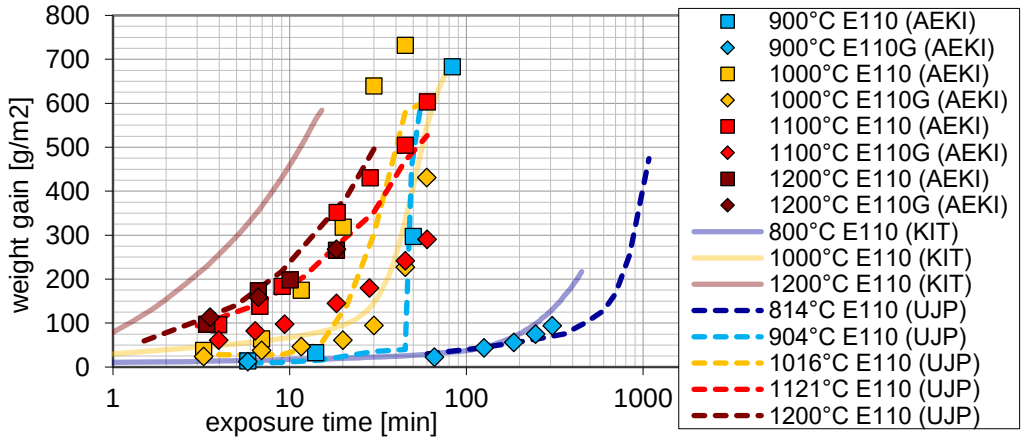

Fig. 12: Weight gain comparison of examined E110 alloy with results of KIT [4] and AEKI [7] experiments with Zircaloy-4 and E110 alloys.

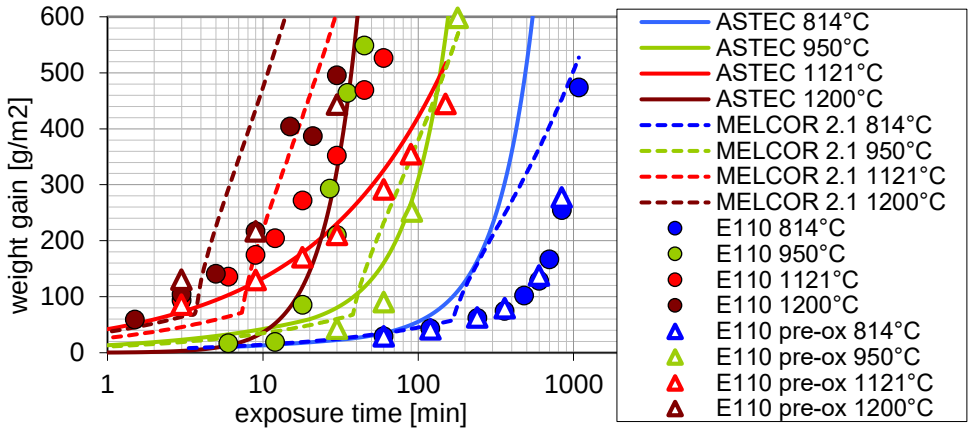

Fig. 13: Weight gain comparison of examined E110 alloy with correlations in computational codes ASTEC and MELCOR 2.1.

Among of alloys in KIT, examined E110 alloy had the lowest weight gain except of critical temperatures 900 °C and 1000 °C. For two lowest investigated temperatures the alloy had approximately same weight gain like M5 alloy. Similar results were gained in comparation with ANL too, but in case of pre-oxidized sets of E110 all other alloys had higher weight gain. High temperature pre-oxidation led to significantly lower weight gain only for 1200 °C in comparison with Zircaloy-4. For 1000 °C there were any differences and for 800 °C the breakaway happened earlier than E110.

It was very difficult to compare results for at-first-sight same alloy E110. However, there are a lot of variants dependent on an exact composition. According to Fig. 12 there were lower weight gain than in KIT but slightly higher one than in AEKI for 1200 °C. Main difference was not observed in reaction rate in pre- or post-breakaway area but in exposure time when the breakaway happened.

A comparison of measured data with computational codes in Fig. 13 were very diverse. For 800 °C both correlations were conservative due to earlier breakaway. For higher temperatures some of them began to be non-conservative. All correlations were developed based on experiments with Zircaloy-4, which has different oxidation behaviour than E110 as it was showed before. Moreover, the source [3] states that MELCOR 2.1 correlations are valid only up to 1000 °C.

5. Discussion

Due to experimental setting there was a problem with weight gain measurement in a few cases of crumbled specimens. So some expositions were repeated. Significant scattering of weight gain at 900 °C and 950 °C is probably caused by various breakaway of particular samples.

Earlier breakaway and higher oxidation were observed on sample edges. It is due to a larger oxidation area and a more inhomogeneity in the oxide layer leading to cracking. Microstructure was examined only in one cross-section. It can give distorted results in case of global oxygen starvation.

In case of in-autoclave pre-oxidation 9,2 μm at 800 °C only one long-time exposition was carried out because any differences were found out.

Two expositions of high-temperature pre-oxidized samples for 3 min at 1200 °C were conducted due to an error. Weight gain of first one was too much high with peeled layer. Second one led to lower weight gain and the oxide layer did not peel. Between points 3 min and 9 min a very similar weight gain was observed probably due to air diffusion delay across the thick dense oxide layer. The high-temperature pre-oxidation was carried out in same

furnace before air exposure by switching gas. Continuing presence of steam for unknown time after switching complicated determination of exposure time. That is why every steam expositions were performed according to same process and thickness of pre-oxidation was determined by measurement.
Measured data were compared with other experiments conducted during integer temperature 700 °C, 800 °C etc. Nevertheless, these values are smaller than used ones in the experiment with E110. That is why conclusions about the least weight gain are eligible.
All weight gains of pre-oxidized E110 were reduced by the weight gain from pre-oxidation because this value significantly influenced comparation mainly for short expositions.

6. Conclusion

High temperature oxidation of sponge-based E110 in air had two different courses – parabolic pre-breakaway and linear post-breakaway. From temperature 1100 °C there were only one course similar to parabolic. Sharp weight gain was observed at 900–1000 °C in post-breakaway area. Pre-oxidation protective effect was confirmed for all temperatures. High temperature pre-oxidation proved to be more protective only at 1200 °C. Axial extension was significant in lower temperatures. Various type of oxide was observed near edges, scratches and during global oxidation starvation. Microstructure was dependent on cross-section position. Nitride grains were visible at higher temperatures. Microstructure and hydrogen content were reflected in mechanical properties. More oxidized samples have less strength, ductility and higher microhardness. Examined E110 alloy oxidized slowly than other compared alloys except of 900–1000 °C. Similar weight gain had M5 alloy in KIT at low temperatures. Given computational codes ASTEC and MELCOR 2.1 were not suitable for oxidation modeling of E110.

7. References

[1] STEINBRÜCK, M.; BÖTTCHER, M.; SCHMET, B.; ENOCH, F. Air oxidation of Zircaloy-4, M5® and ZIRLO™ cladding alloys at high temperatures. Journal of Nuclear Materials [online]. 2011, 414(2), 276-285 [cit. 2018-03-27]. DOI: 10.1016/j.jnucmat.2011.04.012. ISSN 00223115.

[2] NATESAN, K.; SOPPET, W.K. Air Oxidation Kinetics for Zr-Based Alloys. NUREG/CR-6846 ANL-03/32 [online]. 2004 [cit. 2018-03-27].

[3] STEMPNIEWICZ, M.M. Air oxidation of Zircaloy, Part 1 – Review of correlations. Nuclear Engineering and Design [online]. 2016, 301, 402-411 [cit. 2018-03-21]. DOI: 10.1016/j.nucengdes.2016.02.042. ISSN 00295493.

[4] STEINBRÜCK, M. STEGMAIER, U. a ZIEGLER, T. Prototypical Experiments on Air Oxidation of Zircaloy-4 at High Temperatures. Wissenschaftliche Berichte FZKA. Karlsruhe: Forschungszentrum Karlsruhe, 2007, (7257), 84. ISSN ISSN 0947-8620.

[5] DURIEZ, C.; DUPONT, T.; SCHMET, B.; ENOCH, F. Zircaloy-4 and M5® high temperature oxidation and nitriding in air. Journal of Nuclear Materials [online]. 2008, 380(1-3), 30-45 [cit. 2017-04-07]. DOI: 10.1016/j.jnucmat.2008.07.002. ISSN 00223115.

[6] STUCKERT, J., Z. HÓZER, A. KISELEV a M. STEINBRÜCK. Cladding oxidation during air ingress. Part I: Experiments on air ingress. Annals of Nuclear Energy [online]. 2016, 93, 4-17 [cit. 2018-05-15]. DOI: 10.1016/j.anucene.2015.12.034. ISSN 03064549.

[7] MATUS, L., VÉR, N., KUNSTÁR, M., HORVÁTH, M., PINTÉR, A., HÓZER, Z., 2008. Summary of Separate Effect Tests with E110 and Zircaloy-4 in High Temperature Air, Oxygen and Nitrogen. AEKI-FL-2008-401-04/01.